scientific reports

Check for updates

OPEN

The prognostic value and biological significance of MRI CE-T1-based radiomics models in CNS5-identified GBM: a multi-center study

Mingwei Zhang[1,2,3,6], Xiaoxia Li[1,2,6], Yang Yang[4,6], Xuezhen Wang[1,2,6], Shan Li[1,2]✉, Qiuyuan Yue[5]✉, Qichun Wei[4]✉ & Jinsheng Hong[1,2,3]✉

Following the publication of the 2021 WHO Classification of Central Nervous System Tumors (CNS5), Following the publication of the 2021 WHO Classification of Central Nervous System Tumors (CNS5), prognostic markers of glioblastoma (GBM) need to be further explored. Radiomics is a non-invasive and reproducible method for the prognostic assessment of multiple solid tumors. This study aimed to explore the prognostic value and biological significance of MRI T1-weighted enhancement (CE-T1) based radiomics in GBM (CNS5). A six-features radiomics prognostic model was created to calculate the radiomics score (RS). High RS (HR = 3.718, 95%CI: 2.222 − 6.220, $P < 0.001$) was an independent risk factor for overall survival (OS). The correlation between RS and OS was externally verified based on the First Affiliated Hospital of Fujian Medical University cohorts ($n = 93$; HR = 2.015, 95% CI: 1.079 − 3.762, $P = 0.028$) and the Second Affiliated Hospital of Zhejiang University School of Medicine cohorts ($n = 126$; HR = 1.779, 95% CI: 1.023 − 3.091, $P = 0.041$). Through biological significance exploration, RS was found to be significantly correlated with DNA repair ($P = 0.009$) and glycolysis ($P = 0.001$) pathway enrichment scores. RS was associated with γδT cell infiltration and the expression of LAG3. The MRI CE-T1 based radiomics models can predict GBM (CNS5) prognosis noninvasively. RS is relevant to DNA repair, and may guide the screening of radiosensitive populations.

Keywords WHO CNS5 classification, Glioblastoma, IDH, MR radiomics, Prognosis

Glioblastoma (GBM) is the most common intracranial primary malignancy and has high incidence and mortality rates[1]. Current treatment for GBM consists of surgical resection, combined with radiotherapy, chemotherapy, electric field therapy (TTF), and targeted therapy[2]. However, the overall prognosis is poor, and the median overall survival (OS) is approximately 15 to 20 months[3]. The 2021 WHO Classification of Central Nervous System Tumors (5th Edition) (CNS5) integrates the histological characteristics and molecular phenotypes of tumors for integrated diagnostics, redefining the above populations as follows: diffuse astrocytoma with histological features (histGBM) and molecular features (molGBM)[4]. Compared with histodiagnosis alone, the integrated diagnostic mode of central nervous system tumors presents clear advantages in guiding clinical diagnosis, although it also increases the cohort heterogeneity and proposes higher requirements for prognosis prediction[5].

Previous studies based on the 2016 WHO Classification of Central Nervous System Tumors (4th Edition) (CNS4) identified IDH wild-typed GBM prognostic factors including age, sex, KPS score, complete surgical resection of the lesion, chemoradiotherapy, *TERT* promoter status, *MGMT* promoter methylation, *EGFR* amplification, and tumor microenvironment[3]. The CNS5 has redefined the GBM population. Currently, there are

[1]Department of Radiotherapy, Cancer Center, The First Affiliated Hospital, Fujian Medical University, Fuzhou 350005, Fujian, China. [2]National Regional Medical Center, Binhai Campus of the First Affiliated Hospital, Fujian Medical University, Fuzhou, Fujian, China. [3]Key Laboratory of Radiation Biology of Fujian Higher Education Institutions, The First Affiliated Hospital, Fujian Medical University, Fuzhou, Fujian, China. [4]Department of Radiation Oncology, The Second Affiliated Hospital, Zhejiang University School of Medicine, Hangzhou 310009, Zhejiang, China. [5]Department of Radiology, Fujian Cancer Hospital & Fujian Medical University Cancer Hospital, Fuzhou 350014, Fujian, China. [6]These authors contributed equally: Mingwei Zhang, Xiaoxia Li, Yang Yang and Xuezhen Wang. ✉email: 48994373@qq.com; circlessoo@sina.cn; qichun_wei@zju.edu.cn; 13799375732@163.com

few studies on the prognostic factors of GBM (CNS5), and classic prognostic markers such as *MGMT* promoter, *TERT* promoter, and *EGFR* have been challenged in GBM (CNS5) populations[6,7]. As most of the indicators need to be evaluated after invasive biopsy or surgical resection, the evaluation results of pathological indicators are often restricted by various factors including the material site, tissue staining, and detecting instrument, with disadvantages such as difficult sampling, high detection costs, and limited popularity. Radiomics can identify features non-invasively that cannot be distinguished by the naked eye, quantify tumor heterogeneity, and eliminate subjective factors. Further advantages of radiomics are cost-effectiveness, convenience, comprehensiveness and reproducibility. Park CJ et al.[8]detected the prognostic role of radiomics signature in patients with low-grade IDH-wild-type glioma by constructing the radiomics prognostic model. Studies have also examined the prognostic role of the radiomics score (RS) in GBM (CNS4). Choi et al.[9]constructed a radiomics prognostic model of patients with GBM including 13 features through LASSO regression, and found that patients with GBM with high RS had poor OS. It is important to establish whether the RS model is applicable to the GBM population redefined under CNS5.

Wang et al.[10] retrospectively analyzed the data of GBM (CNS5) patients to establish a radiomics features model and explore its independent prognostic role for predicting OS. However, the study did not elucidate the biological meaning underlying radiomics, as it was based on a small sample size and had low statistic power, lack of independent external validation, and insufficient confounding adjustments for absence of treatment-related factors. New identified CNS5 GBM is a highly heterogeneous tumor. Hence, the prognostic value of the MR-based radiomics model for the GBM (CNS5) population across different cancer centers warranted to be evaluated.

Using The Cancer Imaging Archive (TCIA) GBM data, radiomics features from the preoperative MRI T1-weighted enhanced (CE-T1) phase tumor area were extracted and a radiomics prognostic model of GBM (CNS5) was established. Two radiotherapy cohorts were utilized to independently verify the prognostic value of the model. This study then used The Cancer Genome Atlas (TCGA) and Repository of Molecular Brain Neoplasia Data (REMBRANDT) databases to explore the biological correlation between RS and DNA repair, glycolysis, and tumor microenvironment. The aims of this study were to establish the radiomics prognostic model for patients with GBM (CNS5), explore the biological meaning of the RS model, and accurately predict patient prognosis to guide personalized diagnosis and treatment.

Materials and methods

Population definitions

GBM (CNS5): Adult-type diffuse gliomas with wildtype *IDH* and intact *ATRX* and wildtype H3, are defined as "Glioblastoma, *IDHw*t, WHO grade 4" with histological features of microvascular proliferation and/or necrosis, or molecular features of *EGFR* amplification and/or the combination of whole chromosome 7 gain and whole chromosome 10 loss (+7/−10) and/or *TERT* promoter mutations. A histological diagnosis of histGBM was made based on the presence of *IDH*-wildtype diffuse gliomas with necrosis or microvascular proliferation. The molGBM was defined as *IDH*-wildtype diffuse astrocytic tumors without the histological features of GBM with any of the following molecular abnormalities: *TERT* promoter mutation, *EGFR* amplification, or chromosomal + 7/−10 copy changes. Astrocytoma, *IDH*-mutant was defined as a diffusely infiltrating IDH-mutant glioma with *ATRX* loss of expression and/or TP53 mutation and absence of 1p/19q co-deletion. *IDH*-mutant astrocytomas are categorized into grades 2, 3, and 4. Grade 4 lesions present with necrosis and/or microvascular proliferation, or *CDKN2A/2B* homozygous deletion. Oligodendroglioma, *IDH*-mutant and 1p/19q-codeleted was defined as the presence of *IDH* mutation, intact *ATRX* and 1p/19q codeletion[2].

Data acquisition

TCGA

Level 3 gene expression profiles (level 3 data) and associated clinicopathological data of patients with GBM were publicly available from TCGA website (https://portal.gdc.cancer.gov/) accessed on 29 August 2022. The simple nucleotide variation data were obtained, analyzed, and visualized using the 'maftools' in R package[11]. Imaging data were downloaded from TCIA database (https://www.cancerimagingarchive.net).

REMBRANDT

RNAseq (https://identifiers.org/geo:GSE108476) and imaging data (https://wiki.cancerimagingarchive.net/display/Public/REMBRANDT) of GBM patients were publicly available from the REMBRANDT.

FJMU

Data of patients with primary GBM (CNS 5) treated from September 2013 to May 2020 in Department of Radiotherapy of the FJMU were collected retrospectively. Pathological diagnoses were reevaluated and confirmed by two pathologists with 10 years of experience from the Pathology Department of the FJMU.

ZJMU

Data of patients with primary GBM (CNS 5) treated from January 2013 to December 2020 in the Department of Radiotherapy of the Second Affiliated Hospital of Zhejiang University School of Medicine (ZJMU) were collected retrospectively. Pathological diagnoses were reevaluated and confirmed by two pathologists with 10 years of experience from the Pathology Department of the ZJMU.

Study population

TCGA

The inclusion criteria were: (1) first diagnosis of glioblastoma, IDH-wildtype, WHO grade 4 (CNS 5); (2) primary glioma; (3) complete preoperative imaging including cranial MRI CE-T1; (4) complete RNA-seq data.

The exclusion criteria were: (1) history of brain surgery or traumatic brain injury; (2) antineoplastic therapy administered before surgery (including radiotherapy, chemotherapy, biotherapy, immunotherapy or targeted therapy); (3) missing data of preoperative MRI, poor-quality images with low signal-to-noise ratios and artifacts, or low-resolution images that could not be used for the delineation of volumes of interest (VOI); (4) incomplete survival data.

REMBRANDT

The inclusion criteria were: (1) first diagnosis of GBM; (2) primary gliomas; (3) complete preoperative imaging including cranial MRI CE-T1; (4) complete RNA-seq data.

The exclusion criteria were: (1) history of brain surgery or traumatic brain injury; (2) antineoplastic therapy administered before surgery (including radiotherapy, chemotherapy, biotherapy, immunotherapy or targeted therapy); (3) missing data of preoperative MRI, poor quality images with low signal-to-noise ratios, artifacts, or low-resolution images that could be used for delineation of VOI; (4) incomplete survival data.

FJMU

The inclusion criteria were: (1) first diagnosis of glioblastoma, IDH-wildtype, WHO grade 4 (CNS 5); (2) primary gliomas; (3) imaging including cranial MRI CE-T1 performed within 2 weeks prior to surgery; (4) patient undergoing postoperative radiotherapy.

The exclusion criteria were: (1) history of brain surgery or traumatic brain injury; (2) antineoplastic therapy performed before surgery (including radiotherapy, chemotherapy, biotherapy, immunotherapy or targeted therapy); (3) missing data of preoperative MRI, poor-quality images with low signal-to-noise ratios and artifacts, or low-resolution images that could not be used for the delineation of VOI; (4) incomplete survival data.

ZJMU

The inclusion criteria were: (1) first diagnosis of glioblastoma, IDH-wildtype, WHO grade 4 (CNS 5); (2) primary gliomas; (3) imaging including cranial MRI CE-T1 performed within 1 weeks prior to surgery; (4) patients undergoing postoperative radiotherapy.

The exclusion criteria were: (1) history of brain surgery or traumatic brain injury; (2) antineoplastic therapy performed before surgery (including radiotherapy, chemotherapy, biotherapy, immunotherapy or targeted therapy); (3) missing data of preoperative MRI, poor quality images with low signal-to-noise ratios, or artifacts, or low-resolution images that could not be used for delineation of VOI; (4) incomplete survival data.

Endpoint definition

The primary endpoint of the study was OS which was estimated from the date of diagnosis to the date of death or the last follow-up.

Radiotherapy regimen

Please refer to Supplementary Text 1 for details.

Radiomics analysis

Image acquisition

All patients underwent MRI before surgery. See the Supplementary Text 2 for details of the scanning parameters.

Image preprocessing

All MR images were preprocessed before VOI segmentation. For details, see Supplementary Text 3 .

VOI segmentation

The principle of VOI segmentation was detailed in Supplementary Text 4.

Feature extraction

Segmentation data were analyzed with Pyradiomics (https://github.com/Radiomics/pyradiomics) to extract radiomic features, that composed of first-order features, volume and shape features, and texture features.

Feature reduction and model building

Please refer to Supplementary Text 5 for details of the feature reduction and model building. And the model constructed was used to calculate the RS.

Biological significance analysis

Biological significance of RS exploration was determined based on MRI and paired RNA-seq data obtained from TCGA and REMBRANDT. The details were present in Supplementary Text 6.

Statistical analysis

A cut-off point was obtained using the "survMisc" package (https://cran.r-project.org/web/packages/survMisc/index.html)[12], and the population was divided into RS-high and RS-low groups. The categorical variables were presented as numbers and percentages (N, %), and the Pearson's Chi-Square test was used for comparison

between RS-high and -low groups. The OS was calculated using the Kaplan-Meier method and compared using the log-rank test. The univariate and multivariate Cox proportional hazards regression models were constructed to determine potential prognostic factors. The interaction analysis was applied to evaluate the risk difference of subgroups. Correlation analysis was performed with the R package "cor.test", and the data were plotted with the R package ggplot2. Correlation coefficients $|r| \geq 0.7$ indicated strong, $0.3 \leq |r| < 0.7$ moderately strong, and $|r| < 0.3$ weak correlations[13]. R version 4.0.1 (R Foundation for Statistical Computing, Vienna, Austria; www.r-project.org) was used for all statistical analysis. All statistical tests were two-sided, and a p-value of $P < 0.05$ was considered significant.

Ethics approval and consent to participate

All procedures involving human participants were performed in accordance with the Declaration of Helsinki. Ethical approval for the First Affiliated Hospital of Fujian Medical University (FJMU) database was obtained from the Branch for Medical Research and Clinical Technology Application, Ethics Committee of First Affiliated Hospital of Fujian Medical University (approval number: MRCTA, ECFAH of FMU [2022]253) and all participants gave written informed consent. No ethical approval nor informed consent was required for the use of TCGA, TCIA, and REMBRANDT public databases.

Results

Study flow chart (Fig. 1).

Radiomics prognostic model building

Preliminary feature screening

Using TCGA and TCIA databases, radiomics features were extracted from the preoperative MRI CE-T1 enhanced tumor region of 195 diffuse gliomas. Of these, 64 were "Astrocytoma, *IDH*-mutant", 45 were "Oligodendroglioma, *IDH*-mutant and 1p/19q-codeleted", 86 were "GBM (CNS5)". A total of 1967 features were extracted. Of the 1967 radiomics features, 1828 (93%) were selected for the following analyses based on screening of reproducibility

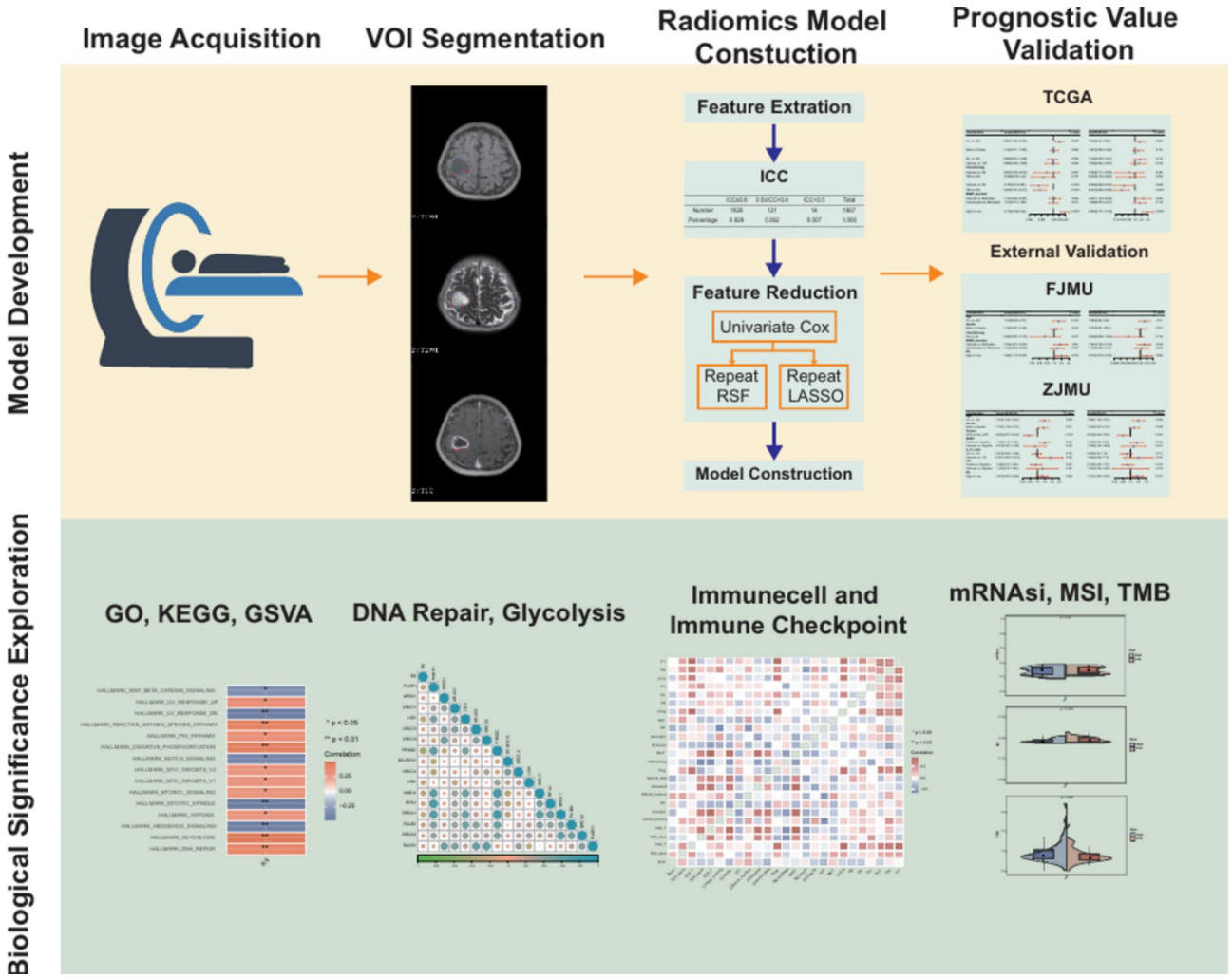

Fig. 1. Study flowchart.

and accuracy, with an average inter-class correlation coefficient (ICC) value of 0.939 and a median ICC value of 0.974. Furthermore, a total of 190 GBM-specific features selected by differential analysis were included in the following analyses.

Feature reduction and model building

First, 32 out of 190 radiomics features were found to be significantly associated with OS as per univariate Cox regression models ($P<0.05$) (Supplementary Table 1). 15 (Supplementary Table 2) and 32 (Supplementary Table 3) features were selected, respectively, for inclusion in Repeat LASSO and Repeat Random Survival Forests (RSF). Finally, 15 features were retained by taking the intersection between two feature sets that were selected using two machine-learning algorithms. Six features out of the features selected above constituted RS model by multivariate Cox proportional hazards model (stepwise regression method). RS was calculated according to the following equation:

RS = 0.336*original_shape_Maximum3DDiameter + 0.647*original_firstorder_Mean + 0.282*original_glrlm_LongRunLowGrayLevelEmphasis + 0.648*wavelet_LLL_glszm_GrayLevelNonUniformity-0.829*exponential_glrlm_LongRunLowGrayLevelEmphasis-0.333*lbp_3D_m1_firstorder_Skewness.

Prognostic value validation

Patient characteristics and survival analysis

A total of 86 patients with GBM (CNS5) were identified. The baseline data were presented in Table 1. A high RS ($P<0.001$) was significantly associated with poor survival in TCGA database as depicted by Kaplan-Meier survival curves (Fig. 2a). A univariate Cox regression model was established to identify potential prognostic factors. We found that high RS (hazard ration [HR] = 3.718, 95% confidence interval [CI]: 2.222 − 6.220, $P<0.001$) and age ≥ 61 (HR = 2.041, 95% CI: 1.269 − 3.284, $P=0.003$) were significantly associated with poor OS, while radiotherapy (YES vs. NO: HR = 0.203, 95% CI: 0.101 − 0.411, $P<0.001$) was a protective factors for OS. RS remained a significant prognostic factor in the multivariate analysis (HR = 3.945, 95% CI: 2.171 − 7.168, $P<0.001$) (Fig. 2b). The results of subgroup analysis in TCGA database were detailed in Fig. 2c.

External validation for prognostic value

The First Affiliated Hospital of Fujian Medical University (FJMU)

The prognostic value of the constructed RS model was further validated using FJMU cohorts. A total of 93 patients with GBM (CNS5) were identified and the baseline data were presented in Supplementary Table 4. A high RS ($P=0.017$) was significantly associated with poor survival as depicted by Kaplan-Meier survival curves (Fig. 3a). Univariate Cox regression model analysis showed that high RS (HR = 1.988, 95% CI: 1.119 − 3.533,

Variables	Total ($n=86$)	High ($n=48$)	Low ($n=38$)	*P*
Age, n (%)				0.184
≤60	44 (51.16)	21 (43.75)	23 (60.53)	
≥61	42 (48.84)	27 (56.25)	15 (39.47)	
Gender, n (%)				0.45
Female	39 (45.35)	24 (50)	15 (39.47)	
Male	47 (54.65)	24 (50)	23 (60.53)	
Group, n (%)				0.005
histoGBM	71 (82.56)	45 (93.75)	26 (68.42)	
molGBM	15 (17.44)	3 (6.25)	12 (31.58)	
KPS, n (%)				0.228
≤80	21 (24.42)	14 (29.17)	7 (18.42)	
>80	50 (58.14)	24 (50)	26 (68.42)	
Unknown	15 (17.44)	10 (20.83)	5 (13.16)	
Chemotherapy, n (%)				0.037
NO	2 (2.33)	2 (4.17)	0 (0)	
Unknown	20 (23.26)	15 (31.25)	5 (13.16)	
YES	64 (74.42)	31 (64.58)	33 (86.84)	
Radiation, n (%)				0.005
NO	10 (11.63)	10 (20.83)	0 (0)	
Unknown	9 (10.47)	4 (8.33)	5 (13.16)	
YES	67 (77.91)	34 (70.83)	33 (86.84)	
MGMT_promoter, n (%)				0.452
Methylated	26 (30.23)	17 (35.42)	9 (23.68)	
Unknown	17 (19.77)	8 (16.67)	9 (23.68)	
Unmethylated	43 (50)	23 (47.92)	20 (52.63)	

Table 1. Patients characteristics in the Cancer Genome Atlas.

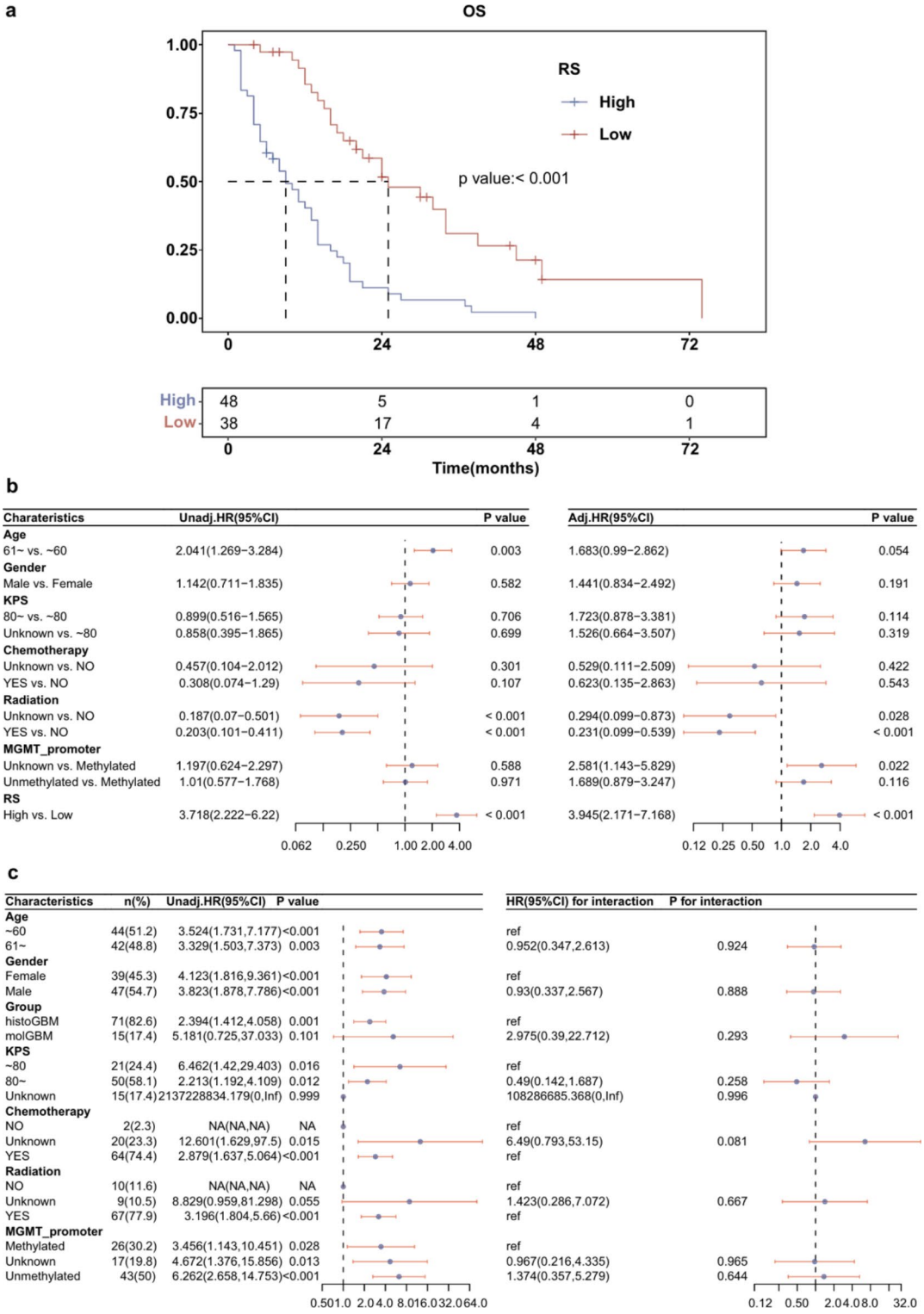

Fig. 2. (**a**) Kaplan-Meier survival curves of radiomics score (RS) based on The Cancer Genome Atlas (TCGA) data (**b**) Forest plots of univariate and multivariate Cox regression analyses of RS based on TCGA data (**c**) Forest plots of subgroup analysis and interaction test between RS and clinicopathological factors based on TCGA data.

$P=0.019$) was significantly associated with poor OS and remained significant in the multivariate analysis (HR = 2.015, 95% CI: 1.079 − 3.762, $P=0.028$) (Fig. 3b). The results of subgroup analysis in FJMU database were detailed in Fig. 3c.

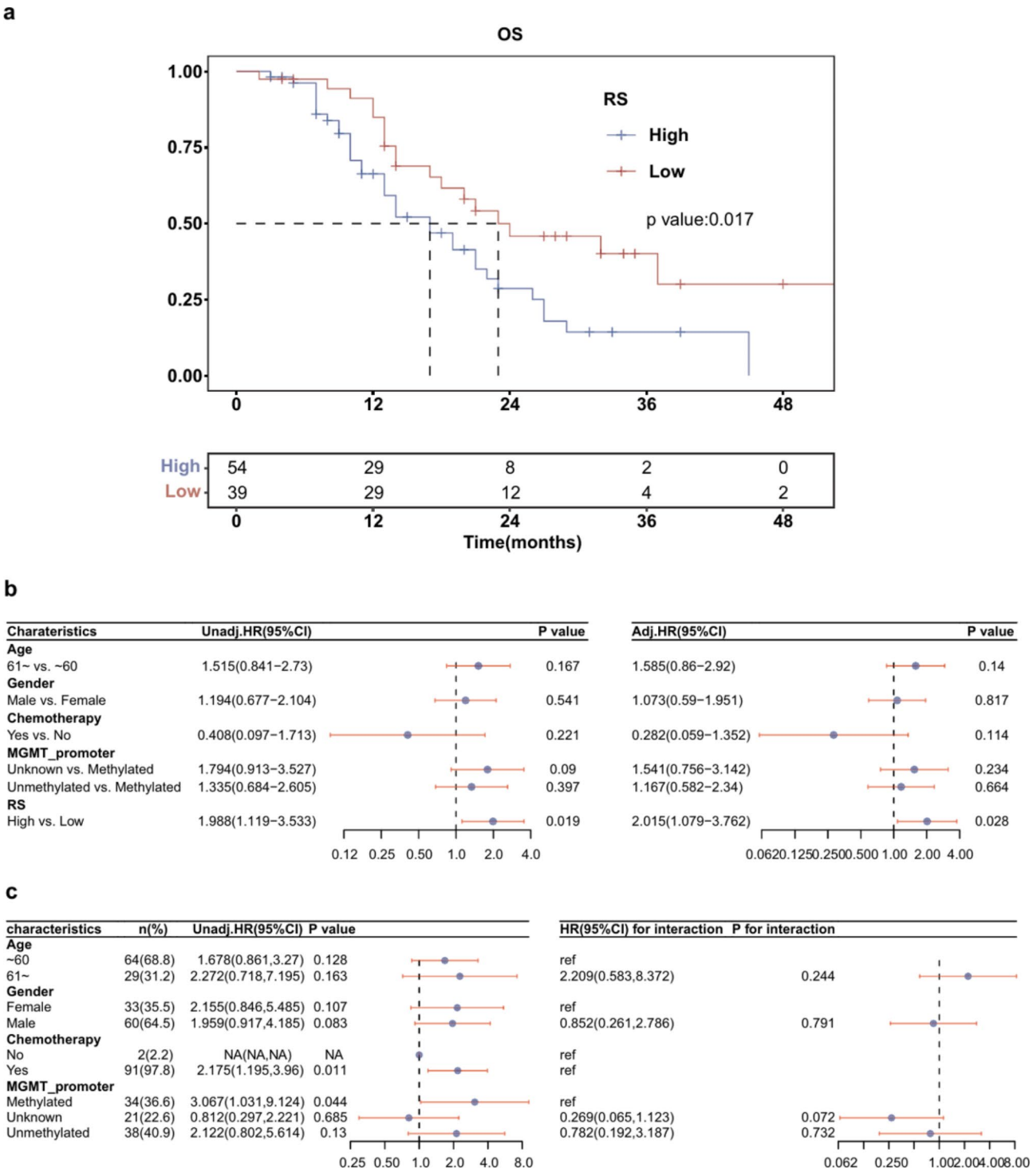

Fig. 3. (**a**) Kaplan-Meier survival curves of radiomics score (RS) based on The First Affiliated Hospital of Fujian Medical University (FJMU) data (**b**) Forest plots of univariate and multivariate Cox regression analyses of RS based on FJMU data (**c**) Forest plots of subgroup analysis and interaction test between RS and clinicopathological factors based on FJMU data.

The Second Affiliated Hospital of Zhejiang University School of Medicine (ZJMU)

The prognostic value of the constructed RS model was further validated using ZJMU cohorts. A total of 126 patients with GBM (CNS5) were identified and the baseline data were summarized in Supplementary Table 5. Kaplan-Meier survival curve analysis showed that there was no significant difference for OS between the RS-high and RS-low groups ($P=0.086$) (Fig. 4a). A univariate Cox regression model analysis showed that age ≥ 61 years (HR = 1.939, 95% CI: 1.236 − 3.041, $P=0.004$), male sex (HR = 1.765, 95% CI: 1.138 − 2.737, $P=0.011$),

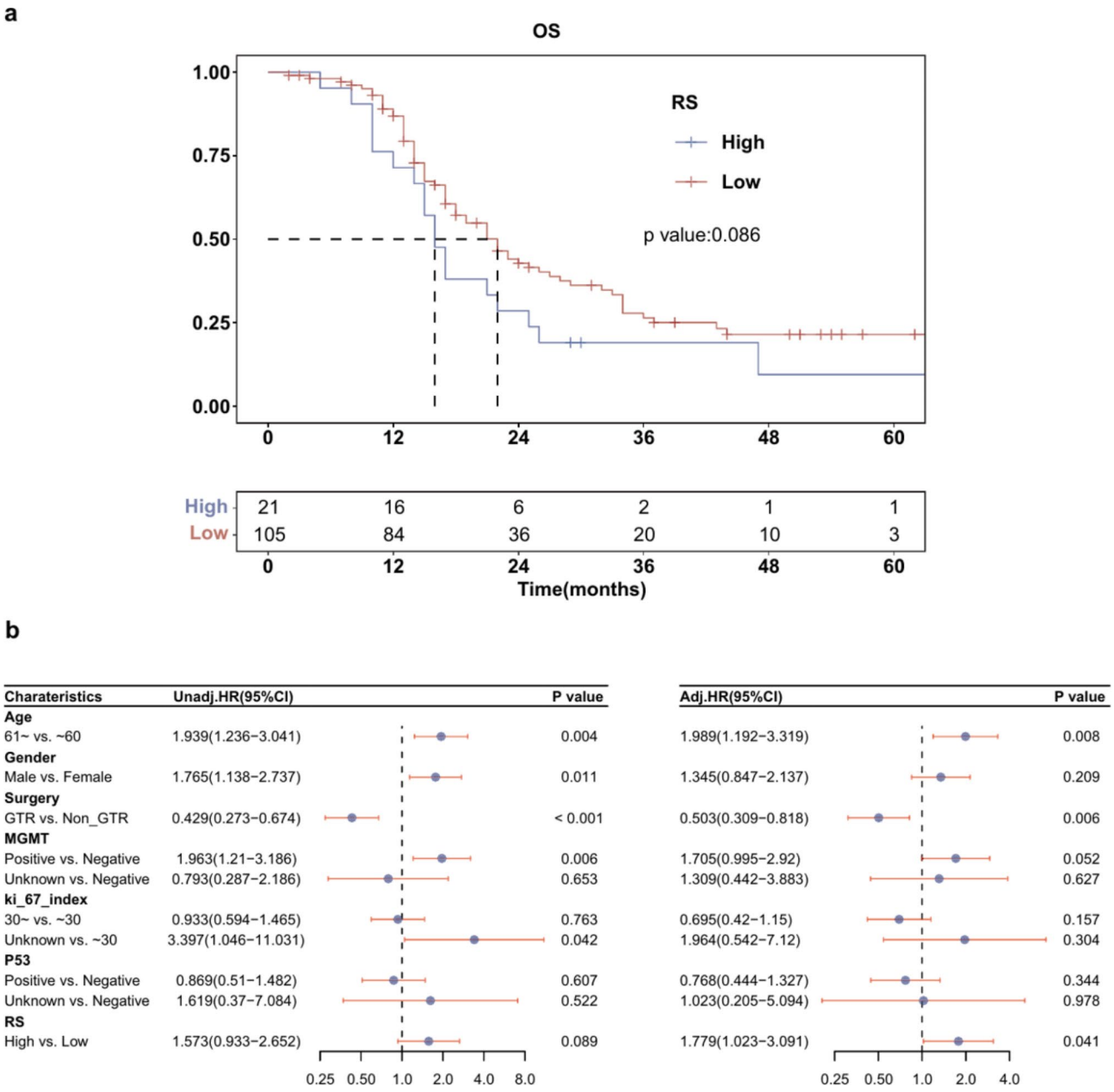

Fig. 4. (**a**) Kaplan-Meier survival curves of radiomics score (RS) based on The Second Affiliated Hospital of Zhejiang University School of Medicine (ZJMU) data (**b**) Forest plots of univariate and multivariate Cox regression analyses of RS based on ZJMU data.

and MGMT protein positive status (HR = 1.963, 95% CI: 1.21 − 3.186, $P = 0.006$) were significant risk factors for OS. Gross total resection (GTR) (HR = 0.429, 95% CI: 0.273 − 0.674, $P < 0.001$) was a protective factor for OS and remained significant in the multivariate analysis (HR = 0.503, 95% CI: 0.309 − 0.818, $P = 0.006$) (Fig. 4b). Multivariable Cox regression analysis demonstrated that High RS (HR = 1.779, 95% CI: 1.023 − 3.091, $P = 0.041$) were independent risk factors for OS (Fig. 4b).

Biological significance analysis

For further exploration of the biological meaning of RS in GBM (CNS5), correlation analyses between RS and genes, signaling pathways, immune cell infiltration, and immune checkpoints were performed based on TCGA database and REMBRANDT database.

TCGA

GO and KEGG enrichment analysis

Gene Ontology (GO) enrichment analysis of differentially expressed genes showed a significant enrichment of the molecular function (MF) category associated with protein serine/threonine kinase activity and of the biological

process (BP) category associated with Ras protein signal transduction and the process utilizing the autophagic mechanism (Supplementary Fig. 1a). Kyoto Encyclopedia of Genes and Genomes (KEGG) enrichment analysis of differentially expressed genes showed a significant enrichment in the MAPK signaling pathway, Wnt signaling pathway and apoptosis pathway (Supplementary Fig. 1b).

GSVA and DNA repair-related and glycolysis-related genes

Gene set variation analysis (GSVA)

The variation score of high RS was positively correlated with DNA repair ($r=0.398$, $P=0.009$), glycolysis ($r=0.484$, $P=0.001$), and the P53 pathway ($r=0.340$, $P=0.028$) and negatively correlated with Wnt/β catenin (r=-0.335, $P=0.031$) (Fig. 5a).

DNA repair-related genes

Correlation analysis between the RS with DNA repair-related genes revealed that RS negatively correlated with *LIG3* (r=-0.321, $P=0.039$) and *PRKDC* (r=-0.426, $P=0.005$) (Fig. 5b).

Glycolysis-related genes

Correlation analysis between the RS with glycolysis-related genes revealed that RS was positively correlated with *ENO3* ($r=0.344$, $P=0.026$), *FAM162A* ($r=0.468$, $P=0.002$) and *B3GAT3* ($r=0.457$, $P=0.003$) (Fig. 5c).

Immune cell infiltration and immune checkpoints

Correlation analysis between the RS with immune infiltrate score revealed that the RS positively correlated with γδT cell infiltration ($r=0.340$, $P=0.028$) (Supplementary Fig. 2a). Correlation analysis between the RS with immune checkpoints indicated that RS was positively correlated with *LAG3* ($r=0.347$, $P=0.025$) (Supplementary Fig. 2b).

TMB, MSI, and mRNAsi

No significant correlation was observed between the RS and mRNA-based stemness index (mRNAsi), microsatellite instability (MSI) and tumor mutation burden (TMB) (Supplementary Fig. 3a-c).

REMBRANDT

GSVA and DNA repair-related and glycolysis-related genes

GSVA The RS positively correlated with DNA repair and glycolysis by GSVA based on the REMBRANDT database. The same trends were observed for TCGA data (Supplementary Fig. 4a).

DNA repair-related genes

Correlation analysis between the RS with DNA repair-related genes revealed that the RS negatively correlated with *LIG3* (r=-0.408, $P=0.076$) (Supplementary Fig. 4b). The trends was observed same as in TCGA data.

Glycolysis-related genes

Correlation analysis between RS with glycolysis-related genes revealed that RS was positively correlated with *FAM162A* ($r=0.468$, $P=0.039$), *ENO3* ($r=0.417$, $P=0.069$), and *B3GAT3* ($r=0.388$, $P=0.092$). Similar trends were observed for TCGA data (Supplementary Fig. 4c).

Immune cell infiltration and immune checkpoints

Correlation analysis between RS with immune infiltrate score revealed the same trend of positive correlation between the RS and the γδT cell as in TCGA database (Supplementary Fig. 5a). And the positive correlation trends between RS and immune checkpoints *LAG3*, *CD48*, *CD70*, *TNFRSF14* were same as those observed in TCGA (Supplementary Fig. 5b).

Discussion

The heterogeneity of the GBM population cohort was recognized under the CNS5 which proposed higher requirements for the determination of patient prognosis. Currently, GBM (CNS5) has limited prognostic predictors, and the vast majority of indicators relies on histological specimen detection. The prognostic value of the MR-based radiomics model in this population has not been established, and the biological meaning of RS in patients with GBM (CNS5) needs to be clarified. In this study, using TCGA and TCIA databases, radiomics features were extracted from the preoperative MRI CE-T1 tumor area, and the radiomics prognostic model of GBM (CNS5) composed of six radiomics features was constructed. A high RS was significantly associated with poor OS. The external data derived from the FJMU and ZJMU bicenter cohorts confirmed the correlation between RS and OS. Moreover, by exploring the correlation between RS and genes, pathways, and immune microenvironment, we found that RS was significantly correlated with the DNA repair pathway and glycolysis pathway and that the RS was associated with immune cell infiltration such as of γδT cells and immune checkpoint expression such as of *LAG3*.

This study found significant association between high RS and poor OS in patients with GBM (CNS5). Previously, RS was found to have good performance in prognosis prediction of different types of cancer. Studies based on MRI radiomics have explored the prognostic value of RS in patients with advanced nasopharyngeal carcinoma, and found that the RS was an adverse prognostic factor for OS (HR = 1.35, 95% CI: 0.98–1.87, $P=0.07$; C-index 0.68 (0.53–0.82))[14]. Similarly, the adverse prognostic effect of high RS has been reported in esophageal cancer[15], cholangiocarcinoma[16]and osteosarcoma[17]. The prognostic role of radiomics models in GBM (CNS4) has been investigated by Choui[9], Sasaki[18], and Zhang[19]. The AUC of prognostic model constructed

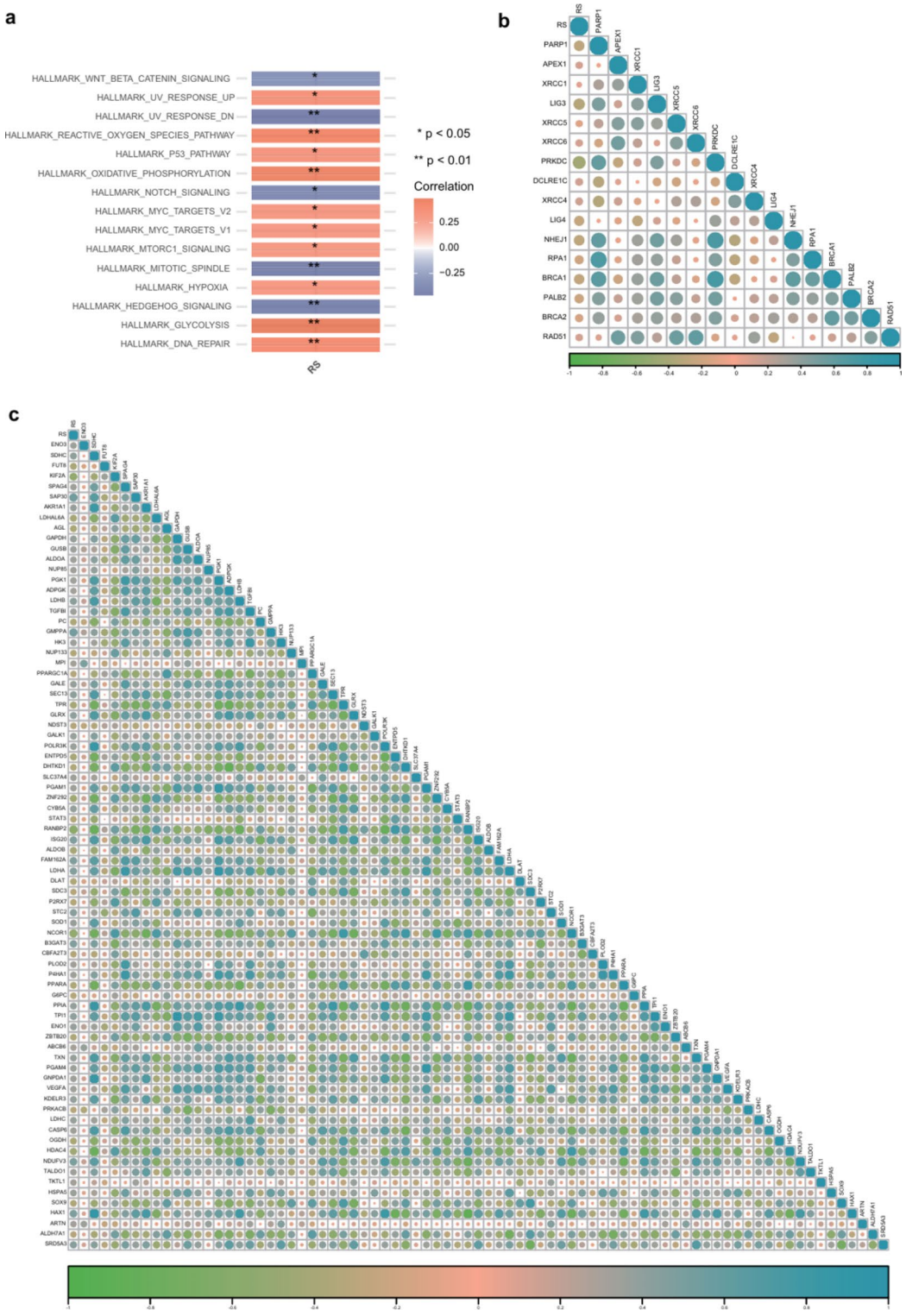

Fig. 5. (**a**) Gene set variation analysis for Hallmark based on The Cancer Genome Atlas (TCGA) data (**b**) Heatmap of correlation analysis between radiomics score (RS) and DNA repair-related genes based on TCGA data (**c**) Heatmap of correlation analysis between RS and glycolysis-related genes based on TCGA data.

by Choui was 0.62 to 0.73, and the radiomics nomogram proposed by Zhang displayed good differentiation of GBM survival stratification in the training (C-index = 0.971) and validation (C-index = 0.974) set. Nevertheless, as CNS5 redefines GBM populations, there are few studies on the predictive prognosis of radiomics in GBM (CNS5) patients. Park et al.[20] found that RS had an independent prognostic factor in molGBM, but the predictive effect of the RS model in GBM (CNS5) remained unclear. Currently, only one study[10] constructed a prognostic

radiomics model composed of eight features based on GBM (CNS5) patients using MRI and public databases. The radiomics model could stratify the risk of patients ($p < 0.001$ and $p < 0.05$ in the training and test sets, respectively), and obtained good prediction consistency (C-index = 0.74–0.86). However, the study was based on a small sample size and had low test efficiency, lack of independent external validation, and did not include tumor treatment factors for multivariate analysis. The present study included multiple factors into analysis and the constructed RS model was associated with OS in patients with GBM (CNS5). External independent validation based on bicenter radiotherapy cohorts verified this association. By exploring the association between RS and GBM (CNS5) prognosis in this study, a comprehensive prognostic model was proposed for patients with strong tumor heterogeneity and difficulty in surgery, and individualized prognosis reference was provided for multidisciplinary diagnosis and treatment quickly and conveniently.

The potential biological significance of radiomics features could significantly enhance its clinical application value. The biological significance of RS based on CNS4 has been previously explored. Park[21] based on CNS4 retrospectively analyzed the NGS detection information and MRI radiomics characteristics of *IDH*wt GBM patients, and constructed an RS model, and discovered that RS had good predictive performance with receptor tyrosine kinase, tumor protein p53 and retinoblastoma 1 pathway, suggesting that RS correlated with invasive biological information. The present study based on the GBM (CNS5) population, explored the biological significance of the constructed RS model.

In this study, RS significantly positively correlated with the DNA repair pathway ($P = 0.009$) through GSVA, and the RS was significantly correlated with *LIG3* and *PRKDC* gene expression by further exploration of the DNA repair-related genes. Previous studies indicated an association between RS and DNA damage repair. Based on the multiple phases of MRI, Huang et al.[22] extracted five features most correlated with *MGMT* promoter methylation in gliomas to construct a radiomics scoring model and found that RS and *MGMT* promoter methylation were significantly correlated. According to a previous study, DNA repair was associated with prognosis. Epigenetic silencing of DNA repair genes was related to tumor formation and response to treatment, and *MGMT* gene promoter methylation affected temozolomide chemotherapy sensitivity and thus prognosis of GBM[23]. DNA damage repair also affected prognosis by causing radiotherapy resistance, and its role in glioma radio-resistance has been demonstrated[24]. Jiang et al.[25] observed that through radiation exposure of glioma cells and mouse models of Valosin protein (VCP) knockout, DNA repair was improved at the cellular level and survival rate was increased, suggesting that VCP enhanced the degradation of DNA-dependent protein kinase catalytic subunit *PRKDC*, resulting in weakened DNA repair and radio-resistance. Other studies have found that *PTEN*[26] enhances radiation resistance by acting on ATMs to inhibit DNA damage repair. *LIG3* was involved in DNA repair by promoting *LIG3-XRCC1*-mediated Okazaki fragment ligation by *PARP1-HPF1*[27]. Moreover, in the present study, RS was significantly positively correlated with the glycolysis pathway ($P = 0.001$), and through further exploration of glycolysis-related genes, High RS was found to be positively correlated with *ENO3*, *FAM162A* expression. Recently, gene expression in patients with high RS was found to be enhanced in glycolysis and other pathways, and some features were strongly positively correlated with glycolysis genes[28]. Li et al.[29] retrospectively analyzed tissue microarrays in patients with glioma and found that high expression of branched-chain amino acid aminotransferase 1 (BCAT1) indicated higher levels of glycolysis, which was associated with malignant progression of *IDH1* wild-type glioma. The unfavorable prognosis associated with glycolysis may be related to the acidic extracellular environment, cellular hypoxia, and angiogenesis caused by aerobic glycolytic upregulation[30], while tumors in oxygen-deprived environments were resistant to radiotherapy. Pursuant to the external validation cohorts of this study, RS was significantly associated with prognosis based on the radiotherapy population, indicating that RS may be a predictor of radio-resistance in GBM (CNS5) patients, providing a non-invasive, reproducible, and cost-effective means for predicting the efficacy of radiotherapy in patients with GBM (CNS5).

This study found that elevated RS was significantly positively correlated with γδT ($P = 0.028$) immune cell infiltration in GBM (CNS5). Previous studies have demonstrated that MR radiomics features correlated with immune cell infiltration[31]. Immune cell infiltration plays a fundamental role in tumor prognosis. In pancreatic ductal adenocarcinoma with γδT cell deletion, the number of CD4 + and CD8 + T cells was increased with upregulation of TNF-α and IFN-γ expression, thereby inhibiting tumor aggressive growth[32]. Studies have also shown that γδT cells could promote the release of cytokine IL-17, thereby inducing an immunosuppressive tumor microenvironment, causing tumor progression[33]. The tumor-promoting effects of γδT cells has also been reported in colon cancer[34] and breast cancer[33]. Moreover, this study indicated that RS positively correlated with *LAG3*, *CD48*, and *CD70* immune checkpoint expression. Previous studies confirmed that RS had a good predictive ability for the expression of PD-1 and PD-L1 in lung cancer patients and for the response to immunotherapy in tumor patients[35,36]. Overexpression of *BACH1* upregulated the expression of glioma cell-derived *LAG3* in vitro, forming an immunosuppressive tumor microenvironment, thus prompting a poor prognosis in GBM[37]. *CD70*[38] is constitutively overexpressed in primary *IDHwt* low-grade glioma and GBM, which is associated with poor prognosis, and may promote tumor migration and macrophage infiltration in GBM[39]. *CD70* has the potential to be a novel CAR target for glioma cancer immunotherapy, and radiomics feature prediction and monitoring follow-up of *CD70* expression could facilitate better screening of the population sensitive to therapy. Zeng[40] et al. found that combining anti-PD-1 therapy and radiotherapy in patients with GBM improved the ratio of CD8 + T cells to Tregs in responders. Immunotherapy provides more opportunities for treatment to patients. Prediction of immune cell infiltration, immune checkpoint expression, and prognosis through non-invasive and convenient individualization of radiomics features offers new approaches for personalized prediction of therapeutic targets and efficacy.

This study presents some limitations. First, despite image standardization, inconsistencies in scanning equipment and image parameters remain between public databases and multi-centers. Second, this study used a single MRI CE-T1, and more features of other MRI sequences should be included for future analysis. Moreover,

subgroup analysis according to different treatments such as anti-vascular targeting and TTF need to be further explored. Specific confounding factors such as type, dose, duration of chemotherapy and radiotherapy, and other medications may result in bias. Also, specific information regarding chemotherapy, such as the chemotherapy regimen, dose, type, and cycle were not recorded in TCGA database and were not available for analysis. Furthermore, the study was a retrospective study, and since *IDH* mutation information was not obtained in the REMBRANDT, the population included in the study was GBM (CNS4) patients. Despite the independent validation of multiple datasets conducted in this study, data from prospective, multicenter, large-sample clinical studies are required to validate our results.

Conclusion

This study demonstrated that a model based on the radiomics features of MRI CE-T1 could predict the prognosis of GBM (CNS5) patients. The model was validated in two independent radiotherapy cohorts. Exploration of the biological significance of the RS model revealed that RS was associated with DNA repair, glycolysis, and immune cell infiltration such as of γδT cells.

Data availability

Data are available from the corresponding authors on reasonable request.

Received: 20 August 2024; Accepted: 4 November 2024
Published online: 11 November 2024

References

1. Ostrom, Q. T. et al. CBTRUS statistical report: primary brain and other central nervous system tumors diagnosed in the United States in 2013–2017. *Neuro Oncol.* **22**, iv1–iv96 (2020).
2. Weller, M. et al. EANO guidelines on the diagnosis and treatment of diffuse gliomas of adulthood. *Nat. Rev. Clin. Oncol.* **18**, 170–186 (2021).
3. Grochans, S. et al. Epidemiology of glioblastoma multiforme-literature review. *Cancers* **14** (2022).
4. Ramos-Fresnedo, A. et al. The survival outcomes of molecular glioblastoma IDH-wildtype: a multicenter study. *J. Neurooncol.* **157**, 177–185 (2022).
5. Louis, D. N. et al. The 2021 WHO classification of tumors of the central nervous system: a summary. *Neuro Oncol.* **23**, 1231–1251 (2021).
6. Galbraith, K. et al. Molecular correlates of long survival in IDH-wildtype glioblastoma cohorts. *J. Neuropathol. Exp. Neurol.* **79**, 843–854 (2020).
7. Mirchia, K., Richardson, T. E. & Beyond IDH-mutation: emerging molecular diagnostic and prognostic features in adult diffuse gliomas. *Cancers* **12** (2020).
8. Park, C. J. et al. Radiomics risk score may be a potential imaging biomarker for predicting survival in isocitrate dehydrogenase wild-type lower-grade gliomas. *Eur. Radiol.* **30**, 6464–6474 (2020).
9. Choi, Y. et al. Radiomics may increase the prognostic value for survival in glioblastoma patients when combined with conventional clinical and genetic prognostic models. *Eur. Radiol.* **31**, 2084–2093 (2021).
10. Wang, S. et al. Radiomics analysis based on magnetic resonance imaging for preoperative overall survival prediction in isocitrate dehydrogenase wild-type glioblastoma. *Front. Neurosci.* **15**, 791776 (2021).
11. Mayakonda, A. & Koeffler, H. P. Maftools: efficient analysis, visualization and summarization of MAF files from large-scale cohort based cancer studies. *BioRxiv*, 052662 (2016).
12. Bae, S. et al. Radiomic MRI phenotyping of glioblastoma: improving survival prediction. *Radiology.* **289**, 797–806 (2018).
13. Yan, Y. et al. Topographic quadrant analysis of peripapillary superficial microvasculature in optic disc drusen. *Front. Neurol.* **12**, 666359 (2021).
14. Bologna, M. et al. Baseline MRI-radiomics can predict overall survival in non-endemic ebv-related nasopharyngeal carcinoma patients. *Cancers* **12** (2020).
15. Chu, F. et al. Development and validation of MRI-based radiomics signatures models for prediction of disease-free survival and overall survival in patients with esophageal squamous cell carcinoma. *Eur. Radiol.* **32**, 5930–5942 (2022).
16. Zhao, J. et al. Development and validation of preoperative magnetic resonance imaging-based survival predictive nomograms for patients with perihilar cholangiocarcinoma after radical resection: a pilot study. *Eur. J. Radiol.* **138**, 109631 (2021).
17. Zhao, S. et al. Radiomics signature extracted from diffusion-weighted magnetic resonance imaging predicts outcomes in osteosarcoma. *J. Bone Oncol.* **19**, 100263 (2019).
18. Sasaki, T. et al. Radiomics and MGMT promoter methylation for prognostication of newly diagnosed glioblastoma. *Sci. Rep.* **9**, 14435 (2019).
19. Zhang, X. et al. A radiomics nomogram based on multiparametric MRI might stratify glioblastoma patients according to survival. *Eur. Radiol.* **29**, 5528–5538 (2019).
20. Park, Y. W. et al. Adding radiomics to the 2021 WHO updates may improve prognostic prediction for current IDH-wildtype histological lower-grade gliomas with known EGFR amplification and TERT promoter mutation status. *Eur. Radiol.* (2022).
21. Park, J. E. et al. Prediction of core signaling pathway by using diffusion- and perfusion-based MRI radiomics and next-generation sequencing in isocitrate dehydrogenase wild-type glioblastoma. *Radiology.* **294**, 388–397 (2020).
22. Huang, W. Y. et al. Radiological model based on the standard magnetic resonance sequences for detecting methylguanine methyltransferase methylation in glioma using texture analysis. *Cancer Sci.* **112**, 2835–2844 (2021).
23. Costello, J. F., Futscher, B. W., Tano, K., Graunke, D. M. & Pieper, R. O. Graded methylation in the promoter and body of the O6-methylguanine DNA methyltransferase (MGMT) gene correlates with MGMT expression in human glioma cells. *J. Biol. Chem.* **269**, 17228–17237 (1994).
24. Meng, W., Palmer, J. D., Siedow, M., Haque, S. J. & Chakravarti, A. Overcoming radiation resistance in gliomas by targeting metabolism and DNA repair pathways. *Int. J. Mol. Sci.* **23** (2022).
25. Jiang, N. et al. Valosin-containing protein regulates the proteasome-mediated degradation of DNA-PKcs in glioma cells. *Cell. Death Dis.* **4**, e647 (2013).
26. McCabe, N. et al. Mechanistic rationale to target PTEN-deficient tumor cells with inhibitors of the DNA damage response kinase ATM. *Cancer Res.* **75**, 2159–2165 (2015).
27. Kumamoto, S. et al. HPF1-dependent PARP activation promotes LIG3-XRCC1-mediated backup pathway of Okazaki fragment ligation. *Nucleic Acids Res.* **49**, 5003–5016 (2021).
28. Liu, Y. et al. Predicting chemo-radiotherapy sensitivity with concordant survival benefit in non-small cell lung cancer via computed tomography derived radiomic features. *Front. Oncol.* **12**, 832343 (2022).

29. Yi, L. et al. Enrichment of branched chain amino acid transaminase 1 correlates with multiple biological processes and contributes to poor survival of IDH1 wild-type gliomas. *Aging (Albany NY)*. **13**, 3645–3660 (2021).
30. Hyder, F. & Khan, M. H. Dysregulated proton and sodium gradients highlight cancer invasion and proliferation. *Transl Oncol.* **16**, 101310 (2022).
31. Li, G. et al. An MRI radiomics approach to predict survival and tumour-infiltrating macrophages in gliomas. *Brain*. **145**, 1151–1161 (2022).
32. Daley, D. et al. Gammadelta T cells support pancreatic oncogenesis by restraining alphabeta T cell activation. *Cell*. **166**, 1485–1499e1415 (2016).
33. Rei, M., Pennington, D. J. & Silva-Santos, B. The emerging protumor role of gammadelta T lymphocytes: implications for cancer immunotherapy. *Cancer Res.* **75**, 798–802 (2015).
34. Hu, G. et al. Tumor-infiltrating CD39(+)gammadeltaTregs are novel immunosuppressive T cells in human colorectal cancer. *Oncoimmunology*. **6**, e1277305 (2017).
35. He, B. et al. Predicting response to immunotherapy in advanced non-small-cell lung cancer using tumor mutational burden radiomic biomarker. *J. Immunother Cancer* **8** (2020).
36. Sun, Z. et al. Radiomics study for predicting the expression of PD-L1 in non-small cell lung cancer based on CT images and clinicopathologic features. *J. Xray Sci. Technol.* **28**, 449–459 (2020).
37. Yuan, F. et al. BACH1 as a potential target for immunotherapy in glioblastomas. *Int. Immunopharmacol.* **103**, 108451 (2022).
38. Jin, L. et al. CD70, a novel target of CAR T-cell therapy for gliomas. *Neuro Oncol.* **20**, 55–65 (2018).
39. Ge, H. et al. Tumor associated CD70 expression is involved in promoting tumor migration and macrophage infiltration in GBM. *Int. J. Cancer*. **141**, 1434–1444 (2017).
40. Zeng, J. et al. Anti-PD-1 blockade and stereotactic radiation produce long-term survival in mice with intracranial gliomas. *Int. J. Radiat. Oncol. Biol. Phys.* **86**, 343–349 (2013).

Acknowledgements

We gratefully acknowledge the financial support from *the Joint Funds for the Innovation of Science and Technology*, *Fujian Province (No. 2021Y9108)* and Beijing xisike Zai Lab Oncology Research Foundation (No. Y-zai2022/qn-0070).

Author contributions

The study design was decided by Mingwei Zhang. Xiaoxia Li wrote the first draft and carried out data extraction and analyses. Yang Yang collected data. Xuezhen Wang carried out data extraction and analyses. Qiuyuan Yue and Shan Li segmented the VOI. Jinsheng Hong and Qichun Wei reviewed the manuscript. All authors contributed to further drafts and approved the final version of the manuscript.

Funding

This research received no external funding.

Declarations

Consent for publication

All authors of this paper have read and approved the final version submitted.

Competing interests

The authors declare no competing interests.

Additional information

Supplementary Information The online version contains supplementary material available at https://doi.org/10.1038/s41598-024-78705-8.

Correspondence and requests for materials should be addressed to S.L., Q.Y., Q.W. or J.H.